Inorg. Chem. **2004**, *43*, 3605–3617

Investigation of Transition Metal–Imido Bonding in $M(NBu^t)_2(dpma)$

James T. Ciszewski, James F. Harrison, and Aaron L. Odom*

Department of Chemistry, Michigan State University, East Lansing, Michigan 48824

Received March 17, 2004

A complete series down group 6 of the formula $M(NBu^t)_2(dpma)$ has been synthesized, where dpma is *N*,*N*-di-(pyrrolyl-α-methyl)-*N*-methylamine. A fourth complex, $Mo(NAr)_2(dpma)$ (**4**), was also prepared, where Ar is 2,6-diisopropylphenyl. All four of these complexes display geometries in the solid state best described as square pyramidal with one imido ligand occupying the axial position and the other an equatorial site. In all cases, the axial imido ligand has a significantly smaller M–N(imido)–C bond angle with respect to the equatorial multiple-bond substituent. From the ^1H, ^{13}C, and ^{14}N NMR spectra, the axial (bent) imido appears to be more electron-rich than the equatorial and linear imido, with the differences becoming less pronounced down the column. The angular deformation energies for the axial imido ligands were studied by DFT in order to discern if and to what extent imido bond angles were important energetically. The electronic energies associated with straightening the axial imido ligand, while holding the remainder of the molecule at the ground-state geometry, for the Cr, Mo, and W derivatives were calculated as 4.5, 2.7, and 2.0 kcal/mol, respectively. A straight-line plot is found for deformation energies versus estimated electronegativity of the group 6 metals in the +6 oxidation state. The study suggests that the electronic differences between metal imido ligands of different angles are quite small; however, the effects may be more pronounced for metal centers with higher electronegativity, e.g. Cr(VI) with electron-withdrawing ligands.

Introduction

In recent years, a resurgence of interest in transition metal−imido complexes has been sparked by new catalytic reactions where NAr is present as a supporting ligand,[1] highly reactive early metal imido compounds that participate in C−H activation,[2] catalytic formation of C−N bonds with titanium imido intermediates,[3] and other processes.[4] Bis(imido) complexes of group 6 have been extensively explored and offer a rich chemistry.[5] In the solid state, many group 6 bis(imido) complexes possess nonequivalent imido substituents where one imido is significantly bent with respect to the other (vide infra). The classic example of a bent imido is found in $Mo(NPh)_2(S_2CNEt_2)_2$,[6] which has two different

* Author to whom correspondence should be addressed. E-mail: odom@cem.msu.edu.

(1) (a) Buchmeiser, M. R. *Chem. Rev.* **2000**, *100*, 1565−1604. (b) Phillips, A. J.; Abell, A. D. *Aldrichimica Acta* **1999**, *32*, 75−89. (c) Schrock, R. R. *Tetrahedron* **1999**, *55*, 8141−8153. (d) Schrock, R. R. Olefin Metathesis by Well-Defined Complexes of Molybdenum and Tungsten. In *Topics in Organometallic Chemistry*; Fürstner, A., Ed.; Springer: Berlin, 1998; Vol. 1. (e) Jamieson, J. Y.; Schrock, R. R.; Davis, W. M.; Bonitatebus, P. J.; Zhu, S. S.; Hoveyda, A. H. *Organometallics* **2000**, *19*, 925−930. (f) Adams, J. A.; Ford, J. G.; Stamatos, P. J.; Hoveyda, A. H. *J. Org. Chem.* **1999**, *64*, 9690−9696. (g) Nugent, W. A.; Feldman, J.; Calabrese, J. C. *J. Am. Chem. Soc.* **1995**, *117*, 8992−8998. (h) La, D. S.; Alexander, J. B.; Cefalo, D. R.; Graf, D. D.; Hoveyda, A. H.; Schrock, R. R. *J. Am. Chem. Soc.* **1998**, *120*, 9720−9721. (i) Alexander, J. B.; La, D. S.; Cefalo, D. R.; Hoveyda, A. H.; Schrock, R. R. *J. Am. Chem. Soc.* **1998**, *120*, 4041−4042. (j) Fujimura, O.; Grubbs, R. H. *J. Org. Chem.* **1998**, *63*, 824−832. (k) Schrock, R. R. *Acc. Chem. Res.* **1990**, *23*, 158−165.

(2) Bennett, J. L.; Wolczanski, P. T. *J. Am. Chem. Soc.* **1997**, *119*, 10696−10719.

(3) For examples, see: (a) Cao, C.; Ciszewski, J. T.; Odom, A. L.*Organometallics* **2001**, *20*, 5011−5013; *Organometallics* **2002**, *21*, 5148. (b) Shi, Y.; Ciszewski, J. T.; Odom, A. L. *Organometallics* **2001**, *20*, 3967−3969; *Organometallics* **2002**, *21*, 5148. (c) Hill, J. E.; Profilet, R. D.; Fanwick, P. E.; Rothwell, I. P. *Angew. Chem., Int. Ed. Engl.* **1990**, *29*, 664. (d) Tillack, A.; Castro, I. G.; Hartung, C. G.; Beller, M. *Angew. Chem., Int. Ed.* **2002**, *41*, 2541. (e) Pohlki, F.; Heutling, A.; Bytschkov, I.; Hotopp, T.; Doye, S. *Synlett* **2002**, 799. (f) Haak, E.; Bytschkov, I.; Doye, S. *Angew. Chem., Int. Ed.* **1999**, *38*, 3389. (g) Johnson, J. S.; Bergman, R. G. *J. Am. Chem. Soc.* **2001**, *123*, 2923. (h) Ackermann, L.; Bergman, R. G. *Org. Lett.* **2002**, *4*, 1475. (i) Ong, T.-G.; Yap, G. P. A.; Richeson, D. S. *J. Am. Chem. Soc.* **2003**, *125*, 8100−8101. (j) Ackermann, L.; Bergman, R. G.; Loy, R. N. *J. Am. Chem. Soc.* **2003**, *125*, 11956−11963. (k) Cao, C.; Shi, Y.; Odom, A. L. *J. Am. Chem. Soc.* **2003**, *125*, 2880−2881.

(4) For a few examples, see: (a) Bruno, J. W.; Li, X. J. *Organometallics* **2000**, *19*, 4672−4674. (b) Zuckerman, R. L.; Bergman, R. G. *Organometallics* **2000**, *19*, 4795−4809. (c) Bashall, A.; Collier, P. E.; Gade L. H.; McPartlin, M.; Mountford P.; Pugh, S. M.; Radojevic, S.; Schubart, M.; Scowen, I. J.; Trosch, D. J. M. *Organometallics* **2000**, *19*, 4784−4794. (d) McInnes, J. M.; Mountford, P. *J. Chem. Soc., Chem. Commun.* **1998**, 1669−1670. (e) Cantrell, G. K.; Meyer, T. Y. *J. Am. Chem. Soc.* **1998**, *120*, 8035−8042.

(5) Wigley, D. E. Organoimido Complexes of the Transition Metals. In *Progress in Inorganic Chemistry*; Karlin, K. D., Ed.; John Wiley & Sons: New York, 1994; Vol. 42, p 239.

10.1021/ic049644o CCC: $27.50
Published on Web 05/12/2004

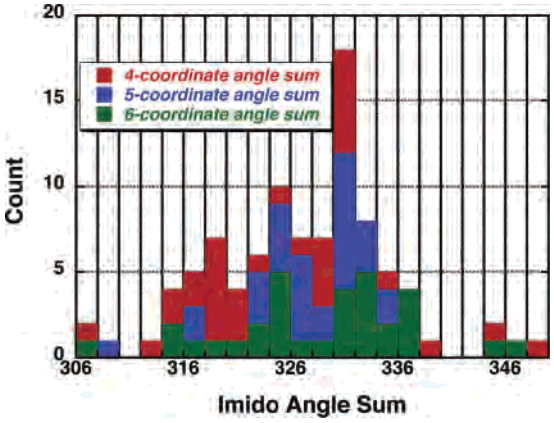

Figure 1. Statistics on the bis(imido) complexes of group 6 from the Cambridge Structural Database. Each entry is the sum of the two imido bond angles in a complex.

Mo−N−Ph angles in the solid state of 169.4(4)° and 139.4(4)°. Although complexes may have very different imido geometries in the solid state, it is rare to find bis(imido) groups that do not equilibrate rapidly in solution, characterized by exchange averaged NMR resonances for the imido groups.[7,8] Alternatively, the distortion existent in the solid state may not persist in fluid solution, which is also consistent with imido group equivalence.

A statistical analysis of the bis(imido) complexes of the group 6 transition elements in the Cambridge Structural Database is shown in Figure 1. In order to avoid problems with determining if a particular imido in a complex was bent relative to another when there may be a partial third bond to both imido ligands, the imido bond angles in each complex were summed. The complex with the lowest sum of bond angles is the aforementioned $Mo(NPh)_2(S_2CNEt_2)_2$ at 309°.[6] The average sum of imido bond angles was 328° with a standard deviation of 8°. In this set, it was no more likely for 6-coordinate complexes, where the maximum bond order to the imido ligands is 2.5, to have smaller imido angles than 4- and 5-coordinate complexes. However, even though 4- and 5-coordinate complexes may have two full triple bonds to the imido ligands, π-bonding to a non-imido ligand may compete with imido π-bonding.[9] Of the bis(imido) complexes examined, 30% had at least one imido with a bond angle of 155° or less. Consequently, imido ligands of group 6 bis(imido) complexes often have fairly small M−N(imido)−C bond angles. A statistical analysis does not suggest, however, anything about whether the imido ligands are bent for electronic reasons nor the energy associated with the bending.

While imido bending is not uncommon in bis(imido) complexes, the extent to which angular deformation is

Chart 1. A Few of the Pertinent Valence Bond Structures for a Transition Metal Bound Imido Ligand

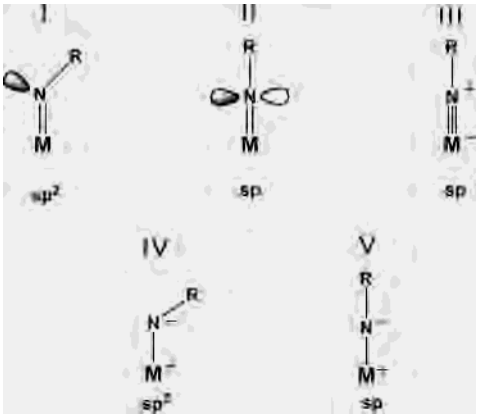

mandated by the electronic structure of most systems is not well established. In addition, imido bending may be of more electronic importance in some systems than in others. In this study, we sought to determine if potential electronic consequences of imido bending were intimately related to electronegativity changes at the metal center and bond polarity.

One commonly discussed bonding model for imido ligands uses three valence bond structures to interpret metal−imido interactions (Chart 1).[5,10] Structure **I** is a bent imido where an sp^2-hybridized nitrogen acts as a 2-electron donor to the metal (using the neutral method for counting electrons). Structure **II** is a linear imido where an sp-hybridized nitrogen acts as a 2-electron donor, and the lone pair of electrons occupies an orbital that is principally N(2p) in character. Structure **III** is a linear imido where an sp-hybridized nitrogen acts as a 4-electron donor with the lone pair on nitrogen donating into a π-acceptor orbital of the metal. Combinations of these three bonding forms have been used to qualitatively categorize metal imido interactions. Among these three canonical forms, structure **I** can be unambiguously identified in the solid state where it is found, but distinction between structures **II** and **III** can be difficult based on metric considerations. Even so, the differences in bonding between structures **II** and **III** clearly have important consequences with respect to the electronics of the system. Although **II** is geometrically similar to **III**, its electron donation more closely resembles mode **I**.

Orbital symmetry arguments have been used to discriminate between **II** and **III**. For example, **II** has been used to describe imido bonding in the complex $Ta(Cp^*)_2(NPh)H$ by Bercaw and co-workers.[11] For a similar niobium phenylimido complex $Nb(Me_3SiCp)_2(NPh)Cl$, the Nb−N−C(ipso) angle is somewhat bent at 165°.[12] Calculations suggest that the potential energy surface describing imido bending is es-

(6) Haymore, B. L.; Maatta, E. A.; Wentworth, R. A. D. *J. Am. Chem. Soc.* **1979**, *101*, 2063.
(7) (a) Barrie, P.; Coffey, T. A.; Forster, G. D.; Hogarth, G. *J. Chem. Soc., Dalton Trans.* **1999**, 4519−4528. (b) Strong, J. B.; Yap, G. P. A.; Ostrander, R.; Liable-Sands, L. M.; Rheingold, A. L.; Thouvenot, R.; Gouzerh, P.; Maatta, E. A. *J. Am. Chem. Soc.* **2000**, *122*, 639−649.
(8) Bradley, D. C.; Hodge, S. R.; Runnacles, J. D.; Hughes, M.; Mason, J.; Richards, R. L. *J. Chem. Soc., Dalton Trans.* **1992**, 1663−1668.
(9) Lin, Z.; Hall, M. B. *Coord. Chem. Rev.* **1993**, *123*, 149.
(10) For the sake of simplicity, we give a few of the canonical valence bond forms. A more complete discussion involving all of the limiting structures as applied to imido bonding is found in the following: Cundari, T. R. *Chem. Rev.* **2000**, *100*, 807−818 and references therein.
(11) Parkin, G.; van Asselt, A.; Leahy, D. J.; Whinnery, L.; Huya, N. G.; Quan, R. W.; Henling, L. M.; Schaefer, W. P.; Santarsiero, B. D.; Bercaw, J. E. *Inorg. Chem.* **1992**, *31*, 82.
(12) Antiñolo, A.; Espinosa, P.; Fajardo, M.; Gómez-Sal, P.; López-Mardomingo, C.; Martin-Alonso, A.; Otero, A. *J. Chem. Soc., Dalton Trans.* **1995**, 1007−1013.

sentially flat to a bond angle of 140°. Consistent with earlier theoretical findings by Jörgenson,[13] electron density in both complexes can be accepted by the phenyl ring reducing imido π-bonding and flattening the potential energy surfaces describing imido angle deformation. For Nb(Cp)$_2$(NBu^t)Cl, a relatively short Nb−N(imido) bond and a linear Nb−N−C(quaternary) angle suggests a structure more closely approximated by **III**.[14]

Calculations suggest that energy differences between linear and bent imido structures are quite small for many complexes,[12,13] a behavior not mirrored by more covalent nitrogen double bonds such as those found in organic imines.[15] Indeed structure **II** is highly reminiscent of the transition state in the "lateral shift" mechanism for imine isomerization, the favored pathway of cis−trans interconversion for most organic imines.[16] A mechanism less likely in more covalent systems involves polarization of the C−N double bond to give a zwitterionic transition state. In transition metal imidos, where the M−N double bond is more highly polarized, the zwitterionic structures should be much larger participants. Consequently, canonical limiting polar forms exemplified by **IV** and **V** (Chart 1) should be considered in the description of transition metal−imido compounds.[10] Interconversion between the two zwitterionic limiting structures causes the bond angle to change dramatically, but electron density at nitrogen and the metal remain relatively constant. As this paper is largely concerned with imido bonding alterations concomitant with electronegativity change at a metal center, some polar forms are included for discussion purposes. Polarity of metal nitrogen bonds increases when descending a triad (vide infra).[17] Consequently, the descriptions **I**, **II**, and **III** should be accompanied by larger contributions from the more polar structures **IV** and **V** for the heavier congeners.

Wilkinson and co-workers prepared Cr(NBu^t)$_2${[Bu^{t}NC(O)]$_2$NBu^t},[18] which exhibits two nonequivalent imido substituents on the NMR time scale in solution.[19] Empirically, it appears that the combination of a tridentate, dianionic ligand and two monodentate substituents on a transition metal often leads to complexes with nonequivalent monodentate groups that do not rapidly exchange, at least on the NMR time scale.[20,21] Utilizing the tridentate, dianionic ligand *N*,*N*-di(pyrrolyl-α-methyl)-*N*-methylamine (dpma), we have synthesized three bis(*tert*-butyl)imido complexes spanning group 6, M(NBu^t)$_2$(dpma). These complexes represent new members of a rare class of bis(imido) complexes where the two imido groups are nonequivalent in fluid solution on the NMR time scale. The three bis(imido) dpma complexes are very closely related structurally and contain two nonequivalent imido groups in the solid state. Consequently, this class is well suited for the study of metal−imido bonding interactions. Because all the members of the triad have structures that are closely related, small differences in the spectroscopy largely are attributed to electronic consequences of proceeding from one metal in group 6 to another. We also have prepared Mo[N(2,6-Pr$^i_2$C$_6$H$_3$)]$_2$(dpma) for comparisons between alkyl and aryl substituents, which will be briefly discussed.

In order to discover what may be learned from this series, the compounds were scrutinized using ^{1}H NMR, ^{13}C NMR, CP-MAS ^{13}C NMR, ^{14}N NMR, and X-ray diffraction. The spectroscopic data were analyzed in a variety of ways to identify the techniques for probing imido electronic structure that are conceptually useful for the system. While the spectroscopic data provide information about imido ligands in differing environments on the same metal, the experimental data cannot distinguish between imido differences due to the dissimilar overall environments and imido geometry, e.g. bond angle. Consequently, density functional theory was used to explore the electronic energy associated with imido bending.

Results and Discussion

Syntheses and Structures. The starting material H$_2$dpma is readily synthesized via Mannich reaction between pyrrole, formaldehyde, and methylamine hydrochloride. Treatment of H$_2$dpma with a slight excess of LiBu^n gives, after workup, Li$_2$dpma.[20]

$$\mathrm{CrBr_2(py)(NBu^t)_2} + \mathrm{Li_2dpma} \xrightarrow[\substack{-2\mathrm{LiBr}\\ -\mathrm{pyridine}\\ 34\%}]{\mathrm{Et_2O}} \underset{\mathbf{1}}{\mathrm{Cr(NBu^t)_2(dpma)}} \quad (1)$$

$$\mathrm{MoCl_2(NBu^t)_2(dme)} + \mathrm{Li_2dpma} \xrightarrow[\substack{-2\mathrm{LiCl}\\ 38\%}]{\mathrm{Et_2O}} \underset{\mathbf{2}}{\mathrm{Mo(NBu^t)_2(dpma)}} \quad (2)$$

$$\mathrm{W(NHBut)_2(NBu^t)_2} + \mathrm{H_2dpma} \xrightarrow[\substack{-2\mathrm{H_2NBu^t}\\ 50\%}]{\mathrm{Et_2O}} \underset{\mathbf{3}}{\mathrm{W(NBu^t)_2(dpma)}} \quad (3)$$

$$\mathrm{MoCl_2(Ndip)_2(dme)} + \mathrm{Li_2dpma} \xrightarrow[\substack{-2\mathrm{LiCl}\\ 35\%}]{\mathrm{Et_2O}} \underset{\mathbf{4}}{\mathrm{Mo(Ndip)_2(dpma)}} \quad (4)$$

Reaction of Cr(NBu^t)$_2$(Br)$_2$(py)[22] and Li$_2$dpma in ethereal solvent yields dark red Cr(NBu^t)$_2$(dpma) (**1**) (eq 1). The

(13) Jørgensen, K. A. *Inorg. Chem.* **1993**, *32*, 1521−1522.
(14) Chernega, A. N.; Green, M. L. H.; Suárez, A. G. *J. Chem. Soc., Dalton Trans.* **1993**, 3031.
(15) McCarty, C. G. *syn-anti* Isomerization and rearrangements. In *The Chemistry of the Carbon−Nitrogen Double Bond*; Patai, S., Ed.; The Chemistry of Functional Groups; Interscience Publishers: London, 1970; p 365−464.
(16) (a) *Cyclic Organonitrogen Stereodynamics*; Lambert, J. B., Takeuchi, Y., Eds.; VCH Publishers: New York, 1992. (b) Guerra, A.; Lunazzi, L. *J. Org. Chem.* **1995**, *60*, 7959−7965. (c) Kontoyianni, M.; Hoffman, A. J.; Bowen, J. P. *J. Comput. Chem.* **1992**, *13*, 57−65.
(17) For an example of recent calculations on oxo systems, see: Gisdakis, P.; Rosch, N. *J. Am. Chem. Soc.* **2001**, *123*, 697−701.
(18) Lam, H.-W.; Wilkinson, G.; Hussain-Bates, B.; Hursthouse, M. B. *J. Chem. Soc., Dalton Trans.* **1993**, 781−788.
(19) For additional systems involving nonexchanging bent and linear imidos on the NMR time scale, see: (a) Danopoulos, A. A.; Wilkinson, G.; Hussain, B.; Hursthouse, M. B. *J. Chem. Soc., Chem. Commun.* **1989**, 896−897. (b) Danopoulos, A. A.; Leung, W.-H.; Wilkinson, G.; Hussain-Bates, B.; Hursthouse, M. B. *Polyhedron* **1990**, *9*, 2625−2634.
(20) Li, Y.; Turnas, A.; Ciszewski, J. T.; Odom, A. L. *Inorg. Chem*. **2002**, *41*, 6298.
(21) Schrock, R. R.; Seidel, S. W.; Schrodi, Y.; Davis, W. M. *Organometallics* **1999**, *18*, 428−437.
(22) Meijboom, N.; Schaverien, C. J.; Orpen, A. G. *Organometallics* **1990**, *9*, 774−782.

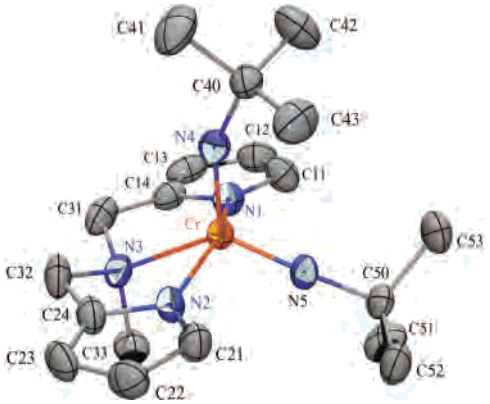

Figure 2. ORTEP representation of the solid-state structure of $Cr(NBu^t)_2$(dpma) (**1**) from X-ray diffraction. Ellipsoids are at the 50% probability level.

solid-state structure exhibits bond angles around chromium inconsistent with either common limiting form for a pentacoordinate complex, but it is best described (vide infra) as a pseudo square pyramid with the imido having the smaller Cr−N(imido)−C bond angle occupying the axial position (Figure 2). Having two different imido substituents, one bent and one linear, is common for bis(imido) complexes in the solid state. Almost invariably, however, the two imido substituents equilibrate in solution, giving rise to a single NMR resonance for the substituents on the imido groups.[7,8] In contrast, there are two sharp, distinct *tert*-butyl resonances observed in the solution ^{1}H NMR of **1** from −80 °C to 80 °C. The chelating dpma ligand apparently prohibits equilibration of the two imido substituents in solution on the NMR time scale.

By reactions outlined in eqs 2 and 3, molybdenum and tungsten analogues of **1**, $Mo(NBu^t)_2$(dpma) (**2**) and $W(NBu^t)_2$(dpma) (**3**), have been synthesized. Molybdenum bis(imido) **2** is readily prepared from $Mo(NBu^t)_2Cl_2$(dme)[23] and Li_2dpma. The tungsten analogue **3** was prepared by transamination on $W(NBu^t)_2(NHBu^t)_2$[24] with H_2dpma. These complexes also display two different resonances due to the *tert*-butylimido groups that do not equilibrate on the ^{1}H NMR time scale even at 80 °C.

The solid-state structures for **1**−**3** are quite similar (Table 1) with the largest variations found in chromium-containing **1** due to its smaller atomic radius. The differences in the imido bond angles for **1**−**3** are slight. The two imido angles in **1** measure 151.1(2)° and 175.3(2)°. The Cr−N(imido) bond distances differ with statistical significance in the chromium derivative at 1.626(2) and 1.641(2) Å for linear and bent, respectively. In the tungsten structure, W−N(imido) distances do not differ with statistical significance at 1.748(3) and 1.757(3) Å. The molybdenum bis(imido) **2** is structurally identical to the tungsten complex **3** within statistical errors for bond distances and angles.

The accuracy of describing complexes **1**−**3** as square pyramids may be quantified using the continuous symmetry parameter $\tau = (\alpha - \beta)/60$, where α and β are the largest and second largest angles around the metal center, respectively.[25] The value of τ can vary from 0 (ideal square pyramid) to 1 (ideal trigonal bipyramid). Consistent with square pyramidal as the closest descriptor for **1**−**3**, τ is computed as 0.28, 0.22, and 0.19, respectively.

Table 1. Selected Bond Distances and Angles from X-ray Diffraction on Complexes **1**−**4**[a]

distances (Å) and angles (deg)	$Cr(NBu^t)_2$(dpma) (**1**)	$Mo(NBu^t)_2$(dpma) (**2**)	$W(NBu^t)_2$(dpma) (**3**)	$Mo[N(2,6\text{-}Pr^i_2C_6H_3)]_2$(dpma) (**4**)
M−N(4)	1.6256(18)	1.731(6)	1.748(3)	1.751(5)
M−N(5)	1.6409(18)	1.732(6)	1.757(3)	1.728(4)
M−N(pyrrolyl) av	1.996(2)	2.068(6)	2.067(3)	2.073(5)
M−N(3)	2.1717(18)	2.339(7)	2.321(3)	2.290(5)
M−N(4)−C	151.10(16)	156.5(6)	158.2(3)	155.8(5)
M−N(5)−C	175.28(16)	171.6(5)	170.4(3)	175.2(5)
N(4)−M−N(5)	112.48(9)	110.5(3)	111.40(14)	111.2(2)
N(pyrrolyl)−M−N(4) av	99.35(8)	104.2(3)	103.57(13)	103.4(2)
N(pyrrolyl)−M−N(5) av	96.64(8)	99.3(3)	99.32(12)	98.1(2)
N(3)−M−N(4)	113.64(8)	98.5(3)	98.89(12)	106.9(2)
N(3)−M−N(5)	133.88(8)	150.8(3)	149.51(12)	141.8(2)
N(pyrrolyl)−M−N(3) av	76.05(8)	72.6(3)	72.57(11)	72.79(18)

[a] For the numbering scheme, see Figure 2.

Arylimido $Mo[N(2,6\text{-}Pr^i_2C_6H_3)]_2$(dpma) (**4**) was prepared from $Mo[N(2,6\text{-}Pr^i_2C_6H_3)]_2Cl_2$(dme)[23] and Li_2dpma in 35% yield (eq 4). X-ray diffraction on **4** yields a structure remarkably similar to the *tert*-butylimido derivative **2**. Arylimido **4** has bent and linear imido angles of 155.8(5)° and 175.2(5)°. The Mo−N(imido) bond distances do vary with statistical significance at 1.728(4) and 1.751(5) Å. The largest difference in the bis(arylimido) structure from those observed for the bis(*tert*-butylimido) complexes is found in the angles to the dpma ligand, which are altered to accommodate the isopropyl substituents. Bis(arylimido) **4** has a structure that closely resembles a square pyramid as judged by the τ-parameter of 0.01 for the solid-state structure.

The $M(imido)_2$ core is remarkably well retained across the entire series as exemplified by the N(4)−M−N(5) bond angles, which are between 110.5° and 112.5° in all four complexes.

^{1}H and ^{13}C NMR Spectroscopy. The ^{1}H and ^{13}C NMR spectra of $M(NBu^t)_2$(dpma), where M = Cr, Mo, and W, display nonequivalent *tert*-butyl resonances. Utilizing NOE experiments, we were able to confirm that the overall geometry in the solid state was retained in solution. Moreover, we were able to determine which resonances in the ^{1}H NMR correspond to the axial (bent) and equatorial (linear) *tert*-butylimido protons for each compound. Once all of the resonances were assigned in the ^{1}H NMR, (^{1}H,^{13}C)-HMQC NMR spectroscopy[26] was used to relate the assignments to the ^{13}C NMR. The full assignments for all of the *tert*-butylimido complexes can be found in the Experimental Section. The NOE experiments confirm what might have been expected; namely, the nuclei near or adjacent to the axial (bent) imido nitrogen are shielded with respect to

(23) Fox, H. H.; Yap, K. B.; Robbins, J.; Cai, S.; Schrock, R. R. *Inorg. Chem.* **1992**, *31*, 2287−2289.
(24) Nugent, W. A.; Harlow, R. L. *Inorg. Chem.* **1980**, *19*, 777−779.
(25) (a) Alvarez, S.; Llunell, M. *Dalton Trans.* **2000**, 3288−3303. (b) Addison, A. W.; Rao, T. N.; Reedijk, J.; van Rijn, J.; Verschoor, G. C. *Dalton Trans.* **1984**, 1349−1356. (c) Zabrodsky, H.; Peleg, S.; Avnir, D. *J. Am. Chem. Soc.* **1992**, *114*, 7843−7851.
(26) Minoretti, A.; Aue, W. P.; Reinhold: M.; Ernst, R. R. *J. Magn. Reson.* **1980**, *40*, 175−190.

comparable nuclei on the equatorial (linear) imido, which is consistent with a more electron-rich nitrogen associated with the axial imido.

Derivatives containing the *tert*-butylimido group enable relatively direct study of M−N bonding by comparison of ^{13}C NMR chemical shifts.[27] This is often accomplished by taking the difference between quaternary and primary carbon resonances in the ^{13}C NMR for the *tert*-butylimido group, which is a quantity referred to here as $\Delta\delta_{\alpha\beta}$. For *tert*-butylimido complexes, the larger values of $\Delta\delta_{\alpha\beta}$ are often attributed to the most covalent metal−nitrogen interactions with the highest amount of triple bond character (structure **III** in Chart 1). Smaller values of $\Delta\delta_{\alpha\beta}$ are believed to be the result of higher electron density on the imido nitrogen, which should be due to greater participation by structures **I**, **II**, **IV**, or **V**. For analogous complexes down a transition metal triad, the polarity increases result in smaller $\Delta\delta_{\alpha\beta}$ values for the heavier congeners, which is consistent with the greater participation of modes **IV** and **V** for isostructural complexes. In our system, polarity increases also result in a smaller $\Delta\delta_{\alpha\beta}$ as one proceeds from chromium to molybdenum to tungsten with values of 47.17, 38.54, and 34.17 ppm, respectively.[28]

While the method of using $\Delta\delta_{\alpha\beta}$ values within an isostructural series to evaluate imido electronics seems to have merit, comparisons between the various ligand sets are tenuous. Disparate ligand geometries naturally lead to different interactions with the imido−metal core and may not accurately describe the $\sigma + \pi$ donor ability of all ligand sets. The utility of the method is as a qualitative estimate of ligand donor ability when used outside of an isostructural series. However, the results with various ligand sets are intriguing and at least consistent with what might be expected intuitively for the donor properties of some common ligand sets.

Many studies demonstrating linear correlations[29] between electronegativities and chemical shifts have appeared in the literature.[30] As may be expected, many of the values for ^{13}C NMR chemical shift differences correlate with estimated electronegativities of the group 6 metals in the +6 oxidation state[31] and thus with expected polarity changes in the metal−nitrogen bonds. Plots of $\Delta\delta_{\alpha\beta}$ versus estimated electronegativity of the metal center for four different bis(*tert*-butylimido) systems are found in Figure 3. The four different systems are M(Tp*)Cl(NBu^t)$_2$,[32] M(OSiR$_3$)$_2$(NBu^t)$_2$,[27,33] M(Cp)Me(NBu^t)$_2$,[22,34] and M(dpma)(NBu^t)$_2$, where M = Cr, Mo, and W. The linear fits for all four lines are quite respectable, suggesting that metal electronegativity is a large contributor to imido nitrogen electron density. The linear fits also suggest that $\Delta\delta_{\alpha\beta}$ values are a reasonable measure of imido nitrogen electron density, at least in isostructural systems. *The good linear fits do not necessarily indicate that Sanderson's electronegativities for M(VI) are accurate but suggest only that the effective electronegativity differences are accurately portrayed within each set of complexes*. In fact, the effective electronegativity of the metal centers in each of the series of complexes should be different. The Sanderson electronegativities were calculated using ligands generally more electronegative and poorer π-donors than most of those represented by this set. Consequently, the Sanderson numbers will overestimate the electronegativity of the metal center. In other words, we have no method for experimentally referencing our plots to give the "true" effective electronegativities on the Pauling scale. However, the more electron-deficient ligand sets would be expected to cause the greatest change in the metal's effective electronegativity and will have the largest slope. The most electron-rich ligand sets should have the smallest slope. The slopes of the lines are consistent with the intuitive ordering of donor ability of the ligand sets. The least electron-donating might be expected to be M(NBu^t)$_2$(Tp*)Cl, which has an 8.87 slope value, with a zwitterionic structure placing a formal positive charge on the metal and an electronegative

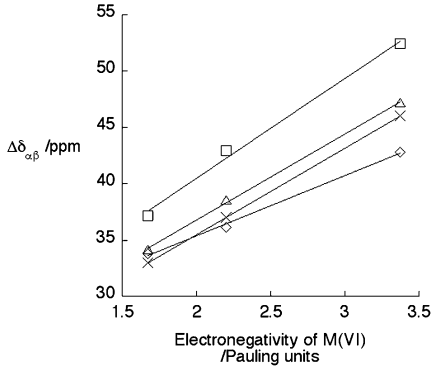

Figure 3. Plot of bis(*tert*-butylimido) complexes of group 6 $\Delta\delta_{\alpha\beta}$ values versus Sanderson electronegativity values for the metals in the +6 oxidation state. □: M(Tp*)Cl(NBu^t)$_2$, $y = 22.785 + 8.8668x$, $R = 0.9974$. △: M(dpma)(NBu^t)$_2$, $y = 21.613 + 7.6024x$, $R = 0.99963$. ×: M(OSiR$_3$)$_2$(NBu^t)$_2$, $y = 20.194 + 7.6545x$, $R = 0.99999$. ◇: M(Cp)(Me)(NBu^t)$_2$, $y = 24.696 + 5.3457x$, $R = 0.99852$.

(27) (a) Nugent, W. A.; McKinney, R. J.; Kasowski, R. V.; Van-Catledge, F. A. *Inorg. Chim. Acta* **1982**, *65*, L91−L93. (b) Ashcroft, B. R.; Clark, G. R.; Nielson, A. J.; Rickard, C. E. F. *Polyhedron* **1986**, *5*, 2081−2091. (c) Nugent, W. A.; Mayer, J. M. *Metal−Ligand Multiple Bonds*; Interscience: New York, 1988; pp 133−135.

(28) The values for the dpma complexes reported were obtained by taking the average of the C_α resonances minus the average of the C_β resonances in each of the spectra. This was done for comparison purposes with other bis(imido) complexes where the imidos are quickly exchanging.

(29) For a discussion and an extensive listing of applications in organic chemistry of NMR as it relates to charge densities, see: Emsley, J. W.; Feeney, J.; Sutcliffe, L. H. *High-Resolution Nuclear Magnetic Resonance Spectroscopy*; Pergamon Press: Oxford, 1966. A brief discussion on paramagnetic contributions to the chemical shift and relevant references are found in the discussion on ^{14}N NMR of this book.

(30) (a) Gasteiger, J.; Marsili, M. *Org. Magn. Reson.* **1981**, *15*, 353−360. (b) Spiesecke, H.; Schneider, W. G. *J. Chem. Phys.* **1961**, *35*, 722−730. (c) Cavanaugh, J. R.; Dailey, B. P. *J. Chem. Phys.* **1961**, *14*, 1099−1107. (d) Dailey, B. P.; Shoolery, J. N. *J. Am. Chem. Soc.* **1955**, *77*, 3977−3981.

(31) For a discussion of Pauling electronegativities versus transition metal oxidation states, see: Sanderson, R. T. *Inorg. Chem.* **1986**, *25*, 3518−3522. The same procedure using optical electronegativities provides plots of equally good linearity. For a discussion of optical electronegativity, see: Jørgensen, C. K. Electron Transfer Spectra. *Prog. Inorg. Chem.* **1971**, *12*, 101. For a similar correlation between optical electronegativity and $\Delta\delta$ values, see ref 27c.

(32) Sundermeyer, J.; Putterlik, J.; Foth, M.; Field, J. S.; Ramesar, N. *Chem. Ber.* **1994**, *127*, 1201. Tp* is tris(3,5-dimethyl-1-pyrazolyl)hydroborate.

(33) For chromium and molybdenum, R is Bu^t. For tungsten, R is Ph.

(34) Radius, U.; Sundermeyer, J. *Chem. Ber.* **1992**, *125*, 2183−2186.

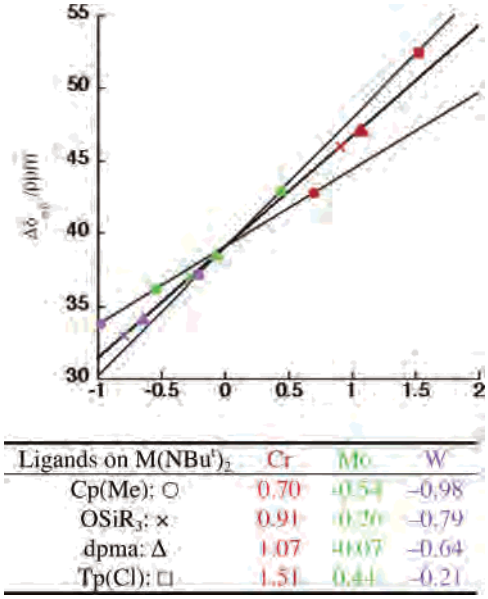

Ligands on $M(NBu^t)_2$	Cr	Mo	W
Cp(Me): ○	0.70	0.54	−0.98
$OSiR_3$: ×	0.91	0.26	−0.79
dpma: Δ	1.07	0.07	−0.64
Tp(Cl): □	1.51	0.44	−0.21

Figure 4. Estimation of electron-withdrawing ability of various ligand sets on $M(NBu^t)_2$. Values are in arbitrary units with bis(*tert*-butyl)diazene as reference of 0. Metal centers estimated to be more electron-withdrawing than the reference are positive.

chlorine atom. The next most electron-deficient ligand set by this measure is $M(NBu^t)_2(OSiR_3)_2$ with a 7.65 slope value, which is very similar to $M(NBu^t)_2$(dpma) with a 7.60 slope value. The most electron-rich ligand set in the series is $M(NBu^t)_2$(Cp)Me with a slope of 5.35, which has quite electron-donating Cp and Me groups.

A method for referencing the $\Delta\delta_{\alpha\beta}$ plots to the Pauling scale is lacking. However, the plots can be referenced to an arbitrary value of $\Delta\delta_{\alpha\beta}$. A natural choice for an arbitrary reference for $Bu^tN{=}M$ complexes is the covalent system bis(*tert*-butyl)diazene, $Bu^tN{=}NBu^t$ ($\Delta\delta_{\alpha\beta} = 39.0$ ppm), where the imido substituent is bound to itself, resulting in a minimum of bond polarity. The results are provided in Figure 4. This reinterpretation of the data in Figure 3 allows estimation of *relative* electron-withdrawing abilities of metal centers in different complexes versus a covalent, double-bond reference. Complexes with positive values presumably would be withdrawing more electron density from the imido nitrogen relative to the reference system, which may be accomplished through triple bonding as in resonance form **III** in Chart 1. Negative values would be found for systems having more participation of polar resonance forms **IV** and **V**. According to this technique, chromium with these ligand sets is always more electron-withdrawing than NBu^t and tungsten less. Molybdenum varied from more to less electron-withdrawing versus the reference depending on the ligand set.

A larger set of ligands, X, in $X_2Cr(NBu^t)_2$ can be examined to estimate the $\sigma + \pi$ donation. For X_2 = (neophyl)$_2$,[22] (neopentyl)$_2$,[22] (benzyl)$_2$,[35] $(OSiMe_3)_2$,[22,27] dpma, and Cl_2[22] the electronic changes result in $\Delta\delta_{\alpha\beta}$ values that range over 14.8 ppm.[36] In other words, altering the other ligands on the group 6 metal can make electronic changes at the imido nitrogens comparable in magnitude to changing the metal center from chromium to tungsten. The effects can be used to estimate the donor ability of the dpma ligand, which is given to be similar to dichloride and bis(trialkylsiloxy).[37]

Differences in solid-state ^{13}C NMR resonances for the *ipso*-carbon of aryl substituents on imido ligands have been successfully correlated to imido bending within $Mo(NR)_2(S_2CNEt_2)_2$ complexes.[7a] For our system in solution, the difference in chemical shift, $\Delta\delta_{l-b}$, for the quaternary carbons on the axial (linear) *tert*-butyl groups minus the equatorial (bent), i.e., $\Delta\delta_{l-b} = C(\alpha)_{linear} - C(\alpha)_{bent}$, was found to change as Cr > W > Mo with $\Delta\delta_{l-b}$ equal to 2.1, 1.3, and 0.8 ppm, respectively.[38] We do not currently have a satisfactory explanation for the observed trend. Despite this, the overall magnitude of $\Delta\delta_{l-b}$ is descriptive. Even though the difference in M−N(imido)−C bond angle is >25° for all the complexes and the two imido substituents reside in distinct coordination positions, the value of $\Delta\delta_{l-b}$ is less than 2.2 ppm, significantly smaller than the effect on $\Delta\delta_{\alpha\beta}$ of changing the metal center or other ligands on the metal.

Consequent to the solution ^{13}C NMR studies, we can discern that imido nitrogen electron density is greatly affected by changes in metal center and other ligands on the metal. The value of $\Delta\delta_{\alpha\beta}$ tracks with the estimated electron-withdrawing ability of the metal center. Imido environment appears to make a measurable but small contribution to the electron density on nitrogen as measured by $\Delta\delta_{l-b}$.

Solid-State ^{13}C NMR Spectroscopy. In order to bridge the gap from the solid-state structural data to the solution-based NMR data, it was desirable to show that the complex in the solid state gives comparable data to solution measurements by some technique. The CP-MAS ^{13}C NMR spectra were obtained, which allowed direct comparison with our solution data. The data correlate amazingly well as can be seen in Table 2. However, some differences between the solution and solid-state data are apparent.

The most interesting feature of the solid-state data involves the $\Delta\delta_{l-b}$ values. The ordering in the solid state was Cr > Mo > W with values of 4.0, 0.9, and 0.8 ppm, respectively. In the solid state, chromium complex **1** has a significantly larger $\Delta\delta_{l-b}$ whereas molybdenum- and tungsten-containing **2** and **3** are similar. In other words, the $\Delta\delta_{l-b}$ values change as Cr > Mo ∼ W using this technique, which is similar to the results found with ^{14}N NMR (vide infra).

^{14}N NMR Spectroscopy. Another tool for investigation of imido bonding is provided by ^{14}N NMR.[39] For example,

(35) Coles, M. P.; Dalby, C. I.; Gibson, V. C.; Clegg, W.; Elsegood, M. R. J. *Chem. Commun.* **1995**, 1709−1711.

(36) For a similar discussion on bis(1-adamantylimido)chromium(VI) complexes, see: Coles, M. P.; Gibson, V. C.; Clegg, W.; Elsegood, M. R. J. *Polyhedron* **1998**, 2483−2489.

(37) Similar results are found when series of molybdenum complexes are examined. Cole, S. C.; Coles, M. P.; Hitchcock, P. B. *Dalton Trans.* **2002**, 4168.

(38) An alternative measure of linear versus bent comparison would be to use $\Delta\delta_{\alpha\beta(linear)} - \Delta\delta_{\alpha\beta(bent)}$. The solution numbers using this method would still go in the order Cr > W > Mo with values of 1.2, 0.7, and 0.1, respectively. However, the result is similar in that the $\Delta\delta$ values due to changing the imido environment are far smaller (<1.2 ppm) than changing the metal or ligands on the metal.

(39) ^{14}N NMR spectra are referenced to the ammonia scale with NH_3 as 0.00 ppm. On this scale, neat nitromethane has a resonance at 380.4 ppm. Another common scale uses ammonium as the reference, which appears at ∼21 ppm on the ammonia scale.

Table 2. Comparison of Solution and Solid-State ^{13}C NMR Data

	Cr(dpma)-(NBu^t)$_2$ (**1**)	Mo(dpma)-(NBu^t)$_2$ (**2**)	W(dpma)-(NBu^t)$_2$ (**3**)
C(*C*H$_3$)$_3$ bent			
solution	30.2	31.0	32.5
solid	30.0	31.0	32.2
C(*C*H$_3$)$_3$ linear			
solution	31.1	31.7	33.1
solid	30.6	32.3	33.6
*C*Me$_3$ bent			
solution	76.8	69.5	66.8
solid	75.8	69.2	66.8
*C*Me$_3$ linear			
solution	78.9	70.3	68.1
solid	79.8	70.1	67.6
*C*H$_2$			
solution	62.9	60.7	60.9
solid	62.3	60.3	59.3
N*C*H$_3$			
solution	46.0	44.6	44.7
solid	44.6	45.2	42.3
pyrrole-4-*C*			
solution	103.0	105.0	105.7
solid	103.2	103.7	106.8
pyrrole-3-*C*			
solution	109.3	110.0	111.0
solid	108.3	109.3	108.9
pyrrole-2-*C*			
solution	132.6	133.4	134.3
solid	132.0	132.4	134.1
pyrrole-1-*C*			
solution	138.9	139.0	139.8
solid	137.1	139.3	140.3

Osborn and Le Ny[40] reported the ^{14}N NMR of several tungsten mono(imido) complexes. The complexes were axially symmetric with trigonal bipyramidal geometries. A consequence of the highly symmetric environment, resonances in the ^{14}N NMR were relatively narrow ($\Delta\nu_{1/2}$ <100 Hz). The lower symmetry of the dpma complexes in our system leads to broader lines; however, all of the resonances corresponding to the nitrogen atoms of the complexes are readily observed.

Shielding in nitrogen NMR is largely ascribed to the paramagnetic term (σ^p) as described by the Ramsey equation.[41] Imido bonding as probed by ^{14}N NMR has been thoroughly discussed by Bradley and co-workers.[8] Imido resonances in nitrogen NMR are known to shield significantly as one proceeds down a column. The shielding is reasonably attributed to higher negative charges on nitrogen as M−N(imido) bond polarity increases and to increases in ΔE due to larger ligand field splittings on proceeding down a column.[8] Nitrogen NMR is expected to be reasonably sensitive to the imido M−N−C angle. For a linear versus bent imido nitrogen, the bent imido will be expected to show decreased ΔE due at least in part to participation of lower energy n $\rightarrow \pi^*$ circulations.[8] Consequently, the less shielded imido nitrogen resonances are attributed to the axial (bent) imido nitrogens.

While all four compounds discussed above display two clearly distinct imido substituents by X-ray crystallography, ^{1}H NMR, and ^{13}C NMR, the imido nitrogens manifest a very different result when interrogated by ^{14}N NMR (Figure 5). The only complex that exhibits two clearly distinct imido resonances is Cr(NBu^t)$_2$(dpma) (**1**). The spectrum of **1** has one relatively sharp peak at 588 ppm ($\Delta\nu_{1/2}$ = 382 Hz) attributable to the axial (bent) imido nitrogen[7b] and a broader resonance at 560 ppm ($\Delta\nu_{1/2}$ = 688 Hz) for the equatorial (linear) imido nitrogen. The molybdenum derivative, Mo(NBu^t)$_2$(dpma) (**2**), was also interrogated by ^{14}N NMR, and evinces two unresolved resonances at 472 ($\Delta\nu_{1/2}$ = 248 Hz) and 458 ppm ($\Delta\nu_{1/2}$ = 1100 Hz). The heaviest congener of the triad, W(NBu^t)$_2$(dpma) (**3**), reveals a single apparent imido resonance at ∼413 ppm. However, simulation of the spectrum requires two resonances at 415 ($\Delta\nu_{1/2}$ = 808 Hz) and 413 ppm ($\Delta\nu_{1/2}$ = 190 Hz) to model the shape of the peak.

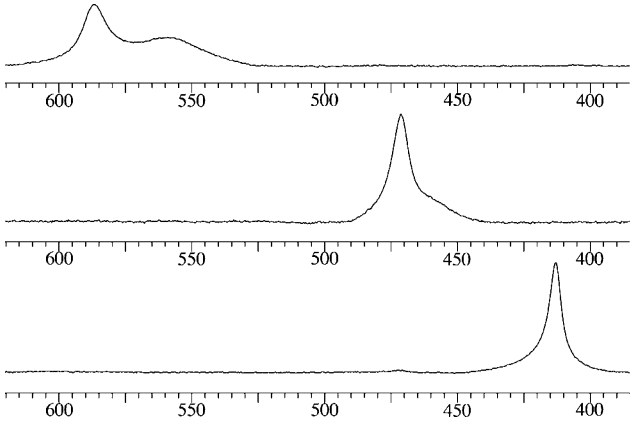

Figure 5. Resonances due to the imido nitrogens in the ^{14}N NMR of Cr(NBu^t)$_2$(dpma) (**1**) [top], Mo(NBu^t)$_2$(dpma) (**2**) [middle], and W(NBu^t)$_2$(dpma) (**3**) [bottom].

As expected, the imido nitrogen resonances do significantly increase in shielding from **1**−**3**. The shielding increase is dramatic at >150 ppm down the triad. Similar trends are seen in the nitrogen NMR of nitrido[42] complexes.[43]

Comparison of the two molybdenum bis(imido) complexes **2** and **4** provides a crude gauge of imido substituent effects on the ^{14}N shift. While alkyl imido **2** displays two resonances for the imido groups, aryl imido **4** has a single peak in the ^{14}N NMR for the imido nitrogen atoms at 429 ppm ($\Delta\nu_{1/2}$ = 648 Hz). Modeling of the imido resonance reveals that the peak shape is Lorentzian. Consequently, it is assumed that the two resonances corresponding to the differentiated imido nitrogens are not separated enough for deconvolution.

One consequence of increased M−N(imido) polarity[31] may be decreased sensitivity of chemical shifts to imido nitrogen environment. This is substantiated by the sensitivity of the ^{14}N resonance shifts to nitrogen environment in the more covalent chromium complex **1**, and lower sensitivity of ^{14}N

(40) Le Ny, J. P.; Osborn, J. A. *Organometallics* **1991**, *10*, 1546−1550.
(41) (a) Webb, G. A.; Witanowski, M. Theoretical Background to Nitrogen NMR. In *Nitrogen NMR*; Witanowski, M., Webb, G. A., Eds.; Plenum Press: London, 1973. (b) Mason, J. *Multinuclear NMR*; Plenum Press: New York, 1987.
(42) (a) Mason, J. *Chem. Rev.* **1981**, *81*, 205−227. (b) Donovan-Mtunzi, S.; Richards, R. L.; Mason, J. *J. Chem. Soc., Dalton Trans.* **1984**, 1329. (c) Dilworth, J. R.; Donovan-Mtunzi, S.; Kan C. T.; Richards, R. L.; Mason, J. *Inorg. Chim. Acta* **1981**, *53*, L161−L162. (d) Odom, A. L.; Cummins, C. C. *Organometallics* **1996**, *15*, 898−900.
(43) For discussion of similar effects in ^{17}O NMR metal−oxo shifts, see: (a) Kidd, R. G. *Can. J. of Chem.* **1967**, *45*, 605−608. (b) Klemperer, W. G. *Angew. Chem., Int. Ed. Engl.* **1978**, *17*, 246−254. (c) Miller, K. F.; Wentworth, R. A. D. *Inorg. Chem.* **1979**, *18*, 984−988.

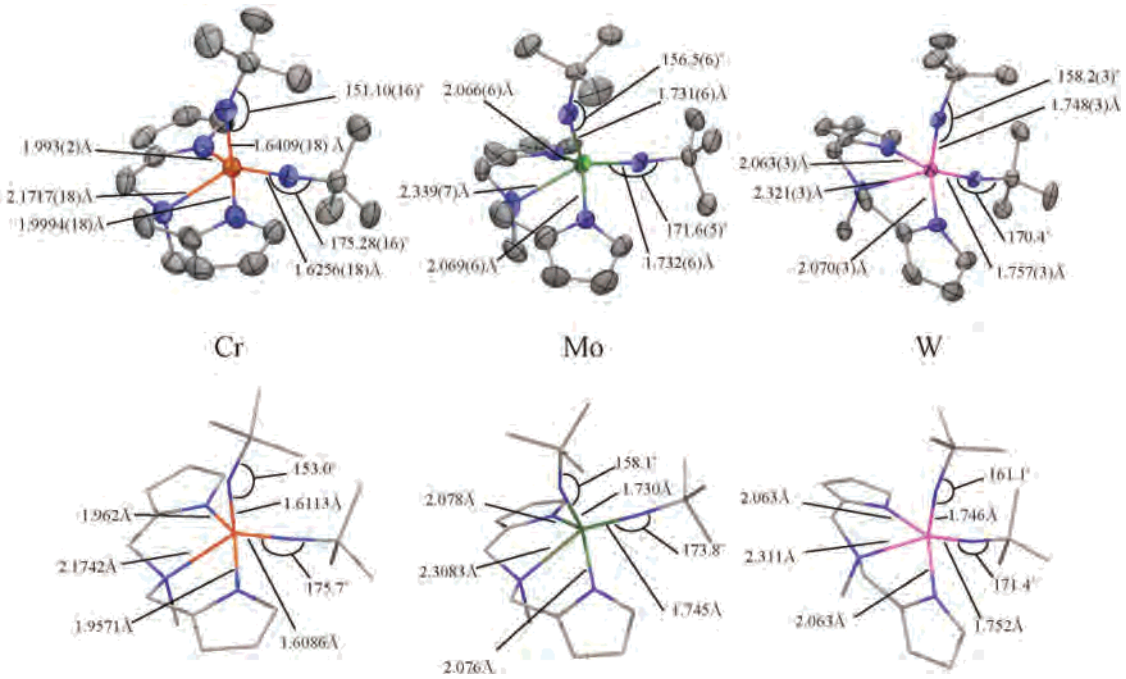

Figure 6. Comparison of bond distances (Å) and angles (deg) from X-ray diffraction (top) on **1**−**3** and the optimized structures from DFT calculations (bottom).

NMR resonance shifts for the more polar tungsten-containing **3**. Indeed, the two imido nitrogens become increasingly difficult to distinguish on proceeding from chromium to molybdenum to tungsten. If one assumes that one of the imido substituents is slightly more electron-rich than the other, which is consistent with the ^{13}C NMR data, the two imido substituents would react slightly differently to decreasing the metal's electronegativity on proceeding down the column. Rising polarity in moving to the heavier congeners effectively decreases the differences in nitrogen shielding in the different environments. A similar argument can be put forth to explain differences between alkyl imido **2** and aryl imido **4**. While two imido peaks are noticeable for **2**, the aryl substituents on the imido nitrogens of **4** result in more electronegative imido nitrogens and higher Mo−N(imido) bond polarity. Consequently, one resonance is observed for the two different imido nitrogens of **4**. In addition, the aryl group will resonance stabilize the imido "lone pair" leading to an increase in ΔE for n $\rightarrow$ π^* paramagnetic circulations, which leads to the ~30 ppm shielding of the arylimido nitrogen relative to the *tert*-butyl derivative.

An alternative explanation would rely on the fact that the major factor leading to differences in ^{14}N NMR chemical shifts is the imido bond angle differences. The other NMR nuclei would need to be more sensitive to other environmental issues. The more polar imido bonds may have a lower energy bent to linear conversion barrier, which is leading to fluxional processes equilibrating the imido bond angles on the ^{14}N NMR time scale. Judging from the solid-state structures and density functional theory calculations (vide infra), the minima of the potential energy surfaces associated with imido bond angle deformation are similar, but the energies associated with a specific angle change are different. One possible experimental probe would be temperature dependence in nitrogen NMR of the complexes. The complexes should all reach a low temperature limit with two nonequivalent imido resonances similar to the chromium structure. Unfortunately, the broadening of the peaks at low temperature quickly becomes prohibitive. On raising the temperature, solutions of **2** gave sharper, clearer resonances with some shifting. However, the shift difference between axial and equatorial imido nitrogen resonances did not change significantly over the temperature range we were able to access. Consequently, there is no fluxionality indicated by the ^{14}N NMR spectra, which is consistent with the spectroscopy of the other nuclei.

From examining ^{14}N NMR of complexes **1**−**3**, a few conclusions may be made. First, the imido nitrogen resonances shield significantly as one proceeds down the triad. Second, lowering the metal's electronegativity has the apparent result of reducing the effective difference between the two imido nitrogens in the two different positions of the square pyramid. Like the $\Delta\delta_{l-b}$ values discussed earlier, the differences between axial (bent) versus equatorial (linear) imido ligands followed the trend Cr > Mo ~ W. However, consistent with the previous spectroscopic results, the shifts due to changing the metal down the triad were substantially larger than due to electronic differences on the two imido ligands.

The ^{14}N NMR resonances corresponding to the amine donors of the dpma region are all in the typical range for amine complexes. Modeling of the tertiary amine peaks gave resonance maximums for compounds **1**−**4** at 84 ($\Delta\nu_{1/2}$ = 1024 Hz), 74 ($\Delta\nu_{1/2}$ = 1594 Hz), 79 ppm ($\Delta\nu_{1/2}$ = 1750 Hz), and 42 ($\Delta\nu_{1/2}$ = 3132 Hz), respectively.

Correlations between ^{14}N NMR chemical shifts of the pyrrolyl nitrogen and π-accepting ability of the transition

metal center would be a potentially useful contribution to metal−pyrrolyl chemistry. Evidence in the literature suggests an intimate link between pyrrole nitrogen NMR shifts and π-electron density in the ring.[44] For free azoles, ^{14}N NMR chemical shifts were found to vary linearly with calculated π-charge densities (SCF-PPP-MO method) of the aromatic ring. Therefore, as applied to our system, significant perturbations in the π-system due to metal center competition for the pyrrolyl nitrogen lone pair could induce dramatic changes in chemical shifts of pyrrolyl nitrogen resonances.

For Cr(NBu^t)$_2$(dpma) (**1**), the ^{14}N NMR resonance for the pyrrolyl nitrogens is found at 195 ppm ($\Delta\nu_{1/2}$ = 125 Hz). The molybdenum and tungsten pyrrolyl nitrogen shifts are found at 198 ($\Delta\nu_{1/2}$ = 372 Hz) and 201 ppm ($\Delta\nu_{1/2}$ = 421 Hz), respectively. The arylimido-containing **4** has a pyrrolyl nitrogen resonance at 206 ppm ($\Delta\nu_{1/2}$ = 895 Hz). The shifts display a slight deshielding as one proceeds down the triad, which is consistent with slightly more π-bonding between the heavier congeners and the pyrrolyl ring. In addition, it appears that the less electron-donating arylimido groups on **4** lead to additional pyrrolyl nitrogen electron-density donation. However, the differences in chemical shifts are relatively small and suggest only little or no significant bonding differences for this particular series. The relatively small ^{14}N NMR chemical shifts on proceeding down the column may be related to competition for the π-acceptor orbital between the axial imido and the pyrrolyl nitrogen lone pairs, which would strongly attenuate the pyrrolyl nitrogen π-donation relative to complexes where a low energy metal orbital is available to accept the nitrogen electron density.[45]

Examination of M(NBu^t)$_2$(dpma) Using DFT. Examination of the structures of M(NBu^t)$_2$(dpma) complexes by density functional theory provided optimized atomic positions in remarkable agreement with the single-crystal X-ray diffraction experiments. The metal−ligand distances and M−N−C angles for complexes **1**−**3** are shown in Figure 6. Like the distances from X-ray diffraction, the bond distances from chromium to the axial and equatorial imido nitrogens are essentially the same. Correlations between bond distance and bond order seem to rarely be valid. The correlations often break down unexpectedly, and bond distances are the product of many different factors.[9] For example, Rothwell and coworkers were able to show experimentally that metal alkoxide bond angle has no apparent correlation to alkoxide bond distance.[46] Examination of the imido complexes M(NBu^t)$_2$(dpma) provides a similar conclusion. The two M−N(imido) bonds in each molecule seem quite similar despite their different environments.

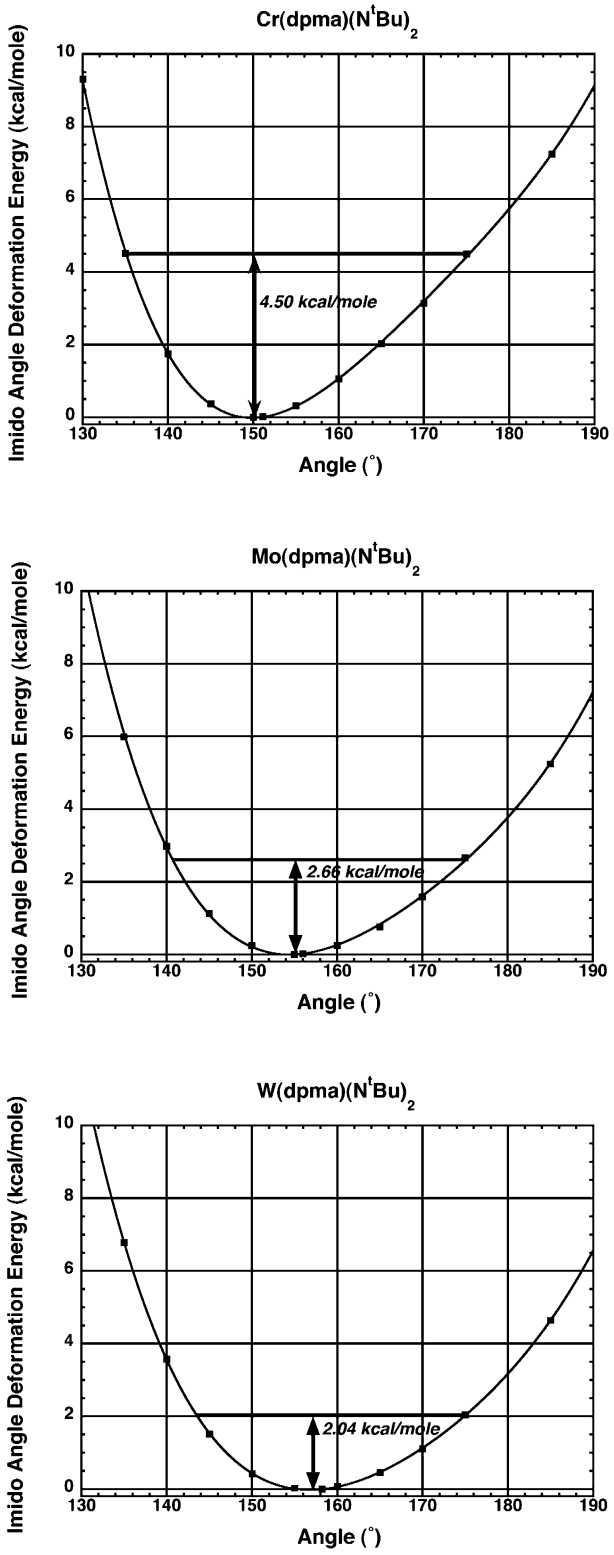

Figure 7. Plots of calculated energies versus angle for the axial imido of compounds **1**−**3**.

(44) Witanowski, M.; Stefaniak, L.; Januszewski, H.; Grabowski, Z. *Tetrahedron* **1972**, *28*, 637−653.

(45) Pyrrolyl ^{14}N NMR chemical shifts for the isostructural series M(dpma)$_2$, where M is Ti, Zr, and Hf, were found to vary over a 47 ppm range. The larger range in these molecules is attributable to stronger π-bond to the metal complexes of this group 4 series with available orbitals, without competing π-donation, to accept π-electron density from the pyrroles. See ref 20.

(46) (a) Steffey, B. D.; Fanwick, P. E., Rothwell, I. P. *Polyhedron* **1990**, *9*, 963−968. For similar examples of early metal alkoxides with little or no correlation between bond distance and angle, see: (b) Howard, W. A.; Trnka, T. M.; Parkin, G. *Inorg. Chem.* **1995**, *34*, 5900. (c) Wolczanski, P. T. *Polyhedron* **1995**, *14*, 3335. For systems where alkoxide bond angle does seem to correlate with bond distance, see: (d) Tomaszewski, R.; Arif, A. M.; Ernst, R. D. *J. Chem. Soc., Dalton Trans.* **1999**, 1883−90. (e) Huffman, J. C.; Moloy, K. G.; Marsella, J. A.; Caulton, K. G. *J. Am. Chem. Soc.* **1980**, *102*, 3009. For a recent computational study supporting Ti−OR triple bonding, see: (f) Dobado, J. A.; Molina, J. M.; Uggla, R.; Sundberg, M. R. *Inorg. Chem.* **2000**, *39*, 2831. For an excellent experimental study comparing π-bonding in a variety of monoanionic ligands to a common metal fragment, see: (g) Lukens, W. W., Jr.; Smith, M. R., III; Andersen, R. A. *J. Am. Chem. Soc.* **1996**, *118*, 1719−1728.

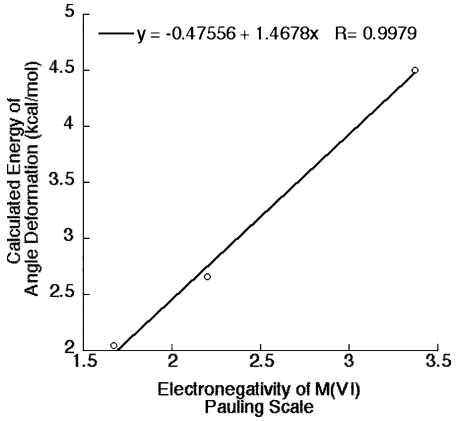

Figure 8. Plot of calculated energy difference from minimum to 175° in axial imido angle versus estimated electronegativities on the Pauling scale.

Using the spectroscopic techniques above, it is not possible to distinguish between different factors leading to resonance differences for the two imido substituents. It was desirable to probe the effect of changing the bond angle on the axial (bent) imido to determine if there is an energetic barrier of some kind associated with the imido bond angle. The energy associated with changing the angle of the axial imido substituent M−N(imido)−C(quaternary Bu^t) to 175°, which is approximately the angle of the equatorial imido, was explored using DFT. The calculations were done by changing the axial imido angle and holding the remainder of the molecule static at the ground-state geometry; this may provide an upper limit on the energy associated with the geometry change. The electronic energy associated with straightening the axial imido for chromium-containing **1** was calculated as 4.5 kcal/mol (Figure 7). A similar calculation by Legzdins and co-workers for imido bending in Cr(O)(NMe)(Me)(NPr^i_2) provided a similar energy associated with Cr−N−C angle deformation of 4.4 kcal/mol.[47] Examination of **2** and **3** using the same technique provided energies for bent imido straightening of 2.7 and 2.0 kcal/mol, respectively.

With energies for imido angle deformation of this magnitude, M−N(imido)−C bond angles should be changing rapidly on the NMR time scale in room temperature solutions. The electronic differences measured in fluid solutions probably represent differences in equilibrium angular values for imido substituents and differences in overall coordination environment.

Interestingly, taking the calculated values for the axial imido angle deformation and plotting versus estimated electronegativity in the +6 oxidation state[31] provided a straight line. This suggests that the angular deformation energy is closely associated with the M−N(imido) bond polarity (Figure 8). If factors other than bond polarity were greatly affecting the electronic energy associated with angle deformation, one might expect the plot in Figure 8 to deviate strongly from linearity.

One question we hoped to address using the calculations was why the axial imido angle deviates from linearity and has a barrier to straightening. If the pyrrolyl substitutents were purely σ-only donors, there would potentially be no electronic reason for the axial imido M−N(imido)−C angle to deviate from linearity. However, any π-bonding from the pyrrolyl ligands could compete with axial imido π-bonding. Several molecular orbitals were found with contributions from the pyrrolyl π-systems and the axial imido consistent with this assertion. In addition, the ^{14}N NMR resonances for the pyrrolyl nitrogen are suggestive of attenuated π-bonding to those substituents due to competition with the imido (vide supra).

Conclusions

In this study, we sought to quantify the relationship between electronegativity and energy associated with imido angle deformation. While none of the techniques described above were convincing on their own, the self-consistent picture created by the host of techniques employed does seem to imply several conclusions concerning the bis(imido) systems described.

While our studies suggest that the axial imido is bent (solution and solid) and that it is more electron-rich relative to the equatorial imido, they do not necessarily establish causality. In other words, we can show that the axial imido is more electron-rich and that it has a smaller imido angle, but we cannot discern definitively that the axial imido is more electron-rich *because* it is bent rather than having this effect as a product of its environment (axial versus equatorial). However, the assertion that the axial imido is bent due to a larger amount of electron-density (or vice-versa) is reasonable if the canonical forms in Chart 1 are a reasonable description of the bonding and assuming that imido ligands have a propensity to form triple bonds (form **III**, Chart 1) when possible. We will assume that imido bond angle and nitrogen electron-density are related. With this caveat, we offer the following conclusions.

The spectroscopic evidence, which includes ^{1}H, ^{13}C, and ^{14}N NMR, suggests that M(NBu^t)$_2$(dpma) complexes do not exchange imido substituents in fluid solution on those time scales. Consequently, it is possible to study the differences in the two imido nitrogens due to their differing environments spectroscopically. For example, it was found that the more shielded *tert*-butyl resonances in the ^{1}H NMR were associated with the, apparently more electron-rich, axial (bent) imido substituents in complexes **1**−**3**. However, it is likely from the calculated electronic energies associated with imido bending that the imido substituents sweep through large angles in solution and observed differences in the two imido substituents are due to variances in equilibrium positions and different environments, e.g. axial vs equatorial, for the two multiple-bond ligands.

The fact that $\Delta\delta_{l-b}$ is nonzero for each complex suggests that there are indeed different electron densities on imido nitrogens in the axial and equatorial orientations. The value of $\Delta\delta_{l-b}$ in solution and in the solid state changed as Cr > Mo ∼ W, similar to differences between imido nitrogen chemical shifts in the ^{14}N NMR.[48] However, the effects of changing the donor ability of the other ligands or the metal center, as judged by $\Delta\delta_{\alpha\beta}$ values, can be significantly larger

(47) Jandciu, E. W.; Legzdins, P.; McNeil, W. S.; Patrick, B. O.; Smith, K. M. *Chem. Commun.* **2000**, 1809.

than the effects of differing imido environments. Therefore, imido environment on the metal center is likely less important to imido bonding than these metal−nitrogen polarity issues.[49]

With the above points in mind, a relatively simple description of imido bonding for this series is made apparent.[50] Polar forms such as **IV** and **V** will contribute to the bonding. Because these zwitterionic contributors both have a M−N(imido) bond order of one, rehybridization involving exchange of **IV** for **V** or vice versa does not greatly affect the bonding or nitrogen electron density. In this model, the barrier to straightening or bending an imido bond will be determined by the energy required to exchange bent imido covalent form **I** with linear imido forms **II** and **III**, the extent to which the polar forms **IV** and **V** participate, and steric effects. Consequently, one expects that as the M−N(imido) bond becomes more covalent for metal centers with relatively high electronegativity, e.g. chromium(VI) with very electron-withdrawing groups, the barrier to nitrogen rehybridization (bending or straightening) should increase. Consistent with this assertion, density functional theory on the complexes in this study found that the chromium imido complex **1** displays a higher barrier to imido angle deformation than the more polar, isostructural tungsten complex. The linear relationship between calculated barriers and estimated electronegativity suggests that bond polarity is a major factor in determining imido deformation energies.

In highly covalent systems, the barrier to isomerization could potentially approach those in organic imines, which typically range from 15 to >23 kcal/mol.[15,16] Consequently, the conclusions on this system are consistent with the results of other studies that have demonstrated calculable[47] and observable[7] differences in imido bonding associated with imido bending, which are usually small. In addition, study of this system suggests that larger barriers to imido angle deformation due to electronic structure may be found for chromium(VI) or other transition metals where the effective electronegativity more closely approximates that of nitrogen and where the bending is mandated[9] by the electronics of the system, rather than sterics[51] or some other effect.

The slightly higher electron density on the bent imido nitrogens of some complexes in combination with greater nitrogen kinetic accessibility potentially could lead to reaction rate and thermodynamic enhancements relative to linear imido ligands on the same complex. The reactivity differences relative to a linear imido are likely to be more important as M−N(imido) bonding becomes more covalent. However, for many systems, M−N(imido)−C bending may be a slight attenuation acting on the larger effect of metal−nitrogen bond polarity in determining nitrogen electron density,[52] which is largely established by the metal, the metal's formal oxidation state, the other ligands, and the substituent on the imido nitrogen.

Experimental Section

General Considerations. All manipulations of air-sensitive materials were carried out in an MBraun glovebox under an atmosphere of purified nitrogen. Ethereal solvents and pentane were purchased from Aldrich Chemical Co. and distilled from purple sodium benzophenone ketyl. Toluene was purchased from Aldrich Chemical Co., refluxed over molten sodium for at least 2 days, and distilled. Dichloromethane was purchased from Spectrum Chemical Co., refluxed with calcium hydride for at least 2 days, and distilled. NMR solvents were purchased from Cambridge Isotopes Laboratories, Inc. Deuterated benzene was distilled from purple sodium benzophenone ketyl. Deuterated toluene was degassed and dried with neutral activated alumina. NMR solvents were stored in sealed containers equipped with a Teflon stopcock in the drybox prior to use. Spectra were taken on Varian instruments located in the Max T. Rogers Instrumentation Facility. Routine coupling constants are not reported. Alumina, silica, and Celite were dried at >200 °C under dynamic vacuum for at least 12 h and then stored under an inert atmosphere. Cr(NBu^t)$_2$(Br)$_2$(py),[22] Mo[N(2,6-Pr$^i_2$C$_6$H$_3$)]$_2$Cl$_2$(dme),[23] W(NBu^t)$_2$(NHBu^t)$_2$,[24] and Mo(NBu^t)$_2$Cl$_2$(1,2-dimethoxyethane)[23] were prepared by literature methods. H$_2$dpma was prepared by the literature procedure.[20] Bis(*tert*-butyl)diazene was purchased from Aldrich Chemical Co., and spectroscopic examinations were carried out in d_7-toluene by ^{1}H [δ = 1.18 (s, Bu^t)] and ^{13}C NMR [δ = 65.95 *C*(CH$_3$)$_3$, 26.90 C(*C*H$_3$)$_3$]. Combustion analyses were performed by Oneida Research Services in Whitesboro, NY.

Procedure for Density Functional Theory Calculations. The calculated molecular structures were obtained by geometry optimizations at the SCF level using the LANL2dz effective core potential and the associated 3s3p3d basis set[53] for the transition metals Cr, Mo, and W while the all electron 3-21g basis[54] was used for the main group elements (H, C, O and N). The potential energy curves for the axial imido angle were calculated at the DFT level using the B3LYP functional.[55] As the angle was varied, we kept the remainder of the molecule at the optimal SCF geometry, a procedure that may overestimate the barrier for imido angle deformation. All calculations used the Gaussian 98-program[56] as implemented on the Chemistry Departments Silicon Graphics Origin 3400 computer.

(48) Imido bond angle has recently been correlated with ^{95}Mo NMR shielding as well. Minelli, M.; Hoang, M. L.; Kraus, M.; Kucera, G.; Loertscher, J.; Reynolds, M.; Timm, N.; Chiang, M. Y.; Powell, D. *Inorg. Chem.* **2002**, *41*, 5954.

(49) For a reference demonstrating through SCF-Xα-SW analysis the high electron density on even linear imido nitrogens, see: Schofield, M. H.; Kee, T. P.; Anhaus, J. T.; Schrock, R. R.; Johnson, K. H.; Davis, W. M. *Inorg. Chem.* **1991**, *30*, 3595−3604.

(50) Similar arguments relating bond order and bond polarity are put forth in ref 27c, Chapter 2.

(51) Coffey, T. A.; Forster, G. D.; Hogarth, G.; Sella, A. *Polyhedron* **1993**, *12*, 2741−2743.

(52) For an interesting reactivity study on an imido with an extremely small angle, see: Gountchev, T. I.; Tilley, T. D. *J. Am. Chem. Soc.* **1997**, *119*, 12831−12841.

(53) Hay, P. J.; Wadt, W. R. *J. Chem. Phys.* **1985**, *82*, 284.

(54) Gordon, M. S.; Binkley, J. S.; Pople, J. A.; Pietro, W. J.; Hehre, W. J. *J. Am. Chem. Soc.* **1982**, *104*, 2797.

(55) Becke, A. D. *J. Chem. Phys.* **1993**, *98*, 1372.

(56) Frisch, M. J.; Trucks, G. W.; Schlegel, H. B.; Scuseria, G. E.; Robb, M. A.; Cheeseman, J. R.; Zakrzewski, V. G.; Montgomery, J. A., Jr.; Stratmann, R. E.; Burant, J. C.; Dapprich, S.; Millam, J. M.; Daniels, A. D.; Kudin, K. N.; Strain, M. C.; Farkas, O.; Tomasi, J.; Barone, V.; Cossi, M.; Cammi, R.; Mennucci, B.; Pomelli, C.; Adamo, C.; Clifford, S.; Ochterski, J.; Petersson, G. A.; Ayala, P. Y.; Cui, Q.; Morokuma, K.; Salvador, P.; Dannenberg, J. J.; Malick, D. K.; Rabuck, A. D.; Raghavachari, K.; Foresman, J. B.; Cioslowski, J.; Ortiz, J. V.; Baboul, A. G.; Stefanov, B. B.; Liu, G.; Liashenko, A.; Piskorz, P.; Komaromi, I.; Gomperts, R.; Martin, R. L.; Fox, D. J.; Keith, T.; Al-Laham, M. A.; Peng, C. Y.; Nanayakkara, A.; Challacombe, M.; Gill, P. M. W.; Johnson, B.; Chen, W.; Wong, M. W.; Andres, J. L.; Gonzalez, C.; Head-Gordon, M.; Replogle, E. S.; Pople, J. A. *Gaussian 98*, revision A.11.1; Gaussian, Inc.: Pittsburgh, PA, 2001.

Preparation of Li_2dpma. A solution of H_2dpma (5.00 g, 26.4 mmol) in approximately 100 mL of toluene was cooled to near frozen in a liquid nitrogen cold well within the drybox. To the stirring cold solution was slowly added 1.6 M *n*-butyllithium (35 mL, 56 mmol, 2.12 equiv) by pipet. The product precipitated as a white solid during addition. When addition was complete, the solution was stirred for 5 min, and then 100 mL of pentane was added. The solid was collected on a frit and was washed repeatedly with pentane. Drying in vacuo yielded Li_2dpma (5.30 g, 26.4 mmol, ~100%).

Preparation of Cr(NBu^t)$_2$(dpma) (1). A solution of Li_2dpma (0.1006 g, 0.500 mmol) in 5 mL of ether was cooled to near frozen in a liquid nitrogen cold well. This was added to a cold solution of $Br_2Cr(NBu^t)_2(py)$ (0.2163 g, 0.499 mmol) in 5 mL of ether. The resulting solution was allowed to warm to box temperature and stirred for 2 h. The solids formed were filtered off, and ether was removed in vacuo. The residue was recrystallized from ether/pentane, yielding **1** as a dark red powder in 34% yield (0.0655 g, 0.172 mmol). ^{1}H NMR (toluene-d_8): δ = 6.97 (s, 2H, pyrrole-5-H), 6.60 (m, 2H, pyrrole-4-H), 6.37 (m Hz, 2H, pyrrole-3-H), 4.37 (d, J = 12.7 Hz, 2H, N-C*H*H-pyrrole, anti to methyl), 3.57 (d, J = 12.7 Hz, 2H, N-CH*H*-pyrrole, syn to methyl), 2.41 (s, 3H, NCH_3), 1.47 (s, 9H, NC(CH_3)$_3$, linear), 1.14 (s, 9H, NC(CH_3)$_3$, bent). ^{13}C NMR (toluene-d_8): δ = 138.95 (pyrrole-1-C), 132.56 (pyrrole-2-C), 109.33 (pyrrole-3-C), 103.00 (pyrrole-4-C), 78.89 (N*C*Me$_3$, linear), 76.78 (N*C*Me$_3$, bent), 62.88 (methine *C*H$_2$), 46.03 (NCH$_3$), 31.12 (NC(*C*H$_3$)$_3$, linear), 30.22 (NC(*C*H$_3$)$_3$, bent). ^{14}N NMR (benzene-d_6): δ = 587.90 ($\Delta\nu_{1/2}$ = 382.27 Hz), 559.80 ($\Delta\nu_{1/2}$ = 688 Hz), 194.84 ($\Delta\nu_{1/2}$ = 327 Hz), 83.66 ($\Delta\nu_{1/2}$ = 1024 Hz). Anal. Calcd for $C_{19}H_{31}N_5Cr$: C, 59.82; H, 8.19; N, 18.36. Found: C, 60.20; H, 8.22; N, 17.98.

Preparation of Mo(NBu^t)$_2$(dpma) (2). A solution of Li_2dpma (0.2014 g, 1.00 mmol) in a mixture of 5 mL of toluene and 1 mL of ether was cooled in a liquid nitrogen temperature cold well to near frozen. This solution was added to a cold, stirring solution of $Cl_2Mo(NBu^t)_2$(dme) (0.4007 g, 1.00 mmol) in 5 mL of toluene. The reaction solution was allowed to warm to box temperature and stirred for 2 h. The solution was filtered, and volatiles were removed in vacuo. The resulting brown solid was recrystallized from pentane, giving **2** as a yellow solid in 38% yield (0.161 g, 0.378 mmol). ^{1}H NMR (toluene-d_8): δ = 7.09 (s, 2H, pyrrole-5-H), 6.51 (m, 2H, pyrrole-4-H), 6.31 (m, 2H, pyrrole-3-H), 4.28 (d, J = 12.7 Hz, 2H, N-C*H*H-pyrrole, anti to methyl), 3.46 (d, J = 12.7 Hz, 2H, N-CH*H*-pyrrole, syn to methyl), 2.17 (s, 3H, NCH_3), 1.49 (s, 9H, NC(CH_3)$_3$, linear), 1.21 (s, 9H, NC(CH_3)$_3$, bent). ^{13}C NMR (toluene-d_8): δ = 139.00 (pyrrole-1-C), 133.37 (pyrrole-2-C), 110.04 (pyrrole-3-C), 104.96 (pyrrole-4-C), 70.29 (N*C*Me$_3$, linear), 69.51 (N*C*Me$_3$, bent), 60.67 (*C*H$_2$), 44.61 (NCH$_3$), 31.69 (NC(*C*H$_3$)$_3$, linear), 31.04 (NC(*C*H$_3$)$_3$, bent). ^{14}N NMR (23 °C, benzene-d_6): δ = 472 ($\Delta\nu_{1/2}$ = 248 Hz), 458 ppm ($\Delta\nu_{1/2}$ = 1100 Hz), 198.30 ($\Delta\nu_{1/2}$ = 372 Hz), 73.75 ($\Delta\nu_{1/2}$ = 1594 Hz). ^{14}N NMR (59 °C, toluene-d_8): δ = 427.03 ($\Delta\nu_{1/2}$ = 273 Hz), 412.98 ($\Delta\nu_{1/2}$ = 792 Hz), 206.76 ($\Delta\nu_{1/2}$ = 432.76 Hz), 69.58 ($\Delta\nu_{1/2}$ = 1981 Hz). Anal. Calcd for $C_{19}H_{31}N_5Mo$: C, 53.64; H, 7.34; N, 16.46. Found: C, 53.50; H, 7.23; N, 16.38. Mo(NBu^t)$_2$Cl$_2$[57] may also be used in the preparation of **2** with similar results.

Preparation of W(NBu^t)$_2$(dpma) (3). A solution of H_2dpma (0.1902 g, 1.00 mmol) in 5 mL of toluene was cooled to near frozen. The cold solution of ligand was added to a cold solution of W(NBu^t)$_2$(NHBu^t)$_2$ (0.4702 g, 1.00 mmol) in 5 of mL toluene. The resulting solution was allowed to warm to box temperature and stirred for 2 h. Volatiles were removed in vacuo to yield a brown oil. To the oil was added 2 mL of pentane. The solution was stirred for several minutes. Volatiles were again removed, which resulted in a yellow solid. Recrystallization from pentane gave **3** as a tan solid in 50% yield (0.255 g, 0.499 mmol). ^{1}H NMR (toluene-d_8): δ = 7.16 (s, 2H, pyrrole-5-H), 6.38 (m, 2H, pyrrole-4-H), 6.20 (m, 2H, pyrrole-4-H), 4.48 (d, J = 12.6 Hz, 2H, N-C*H*H-pyrrole, anti to methyl), 3.46 (d, J = 12.6 Hz, 2H, N-CH*H*-pyrrole, syn to methyl), 1.94 (s, 3H, NCH_3), 1.45 (s, 9H, NC(CH_3)$_3$, linear), 1.12 (s, 9H, NC(CH_3)$_3$, bent). ^{13}C NMR (toluene-d_8): δ = 139.76 (pyrrole-1-C), 134.35 (pyrrole-2-C), 111.00 (pyrrole-3-C), 105.73 (pyrrole-4-C), 68.06 (N*C*Me$_3$, linear), 66.81 (N*C*Me$_3$, bent), 60.87 (*C*H$_2$), 44.658 (NCH$_3$), 33.08 (NC(*C*H$_3$)$_3$, linear), 32.51 (NC(*C*H$_3$)$_3$, bent). ^{14}N NMR (benzene-d_6): δ = 415.21 ($\Delta\nu_{1/2}$ = 808 Hz), 412.70 ($\Delta\nu_{1/2}$ = 190 Hz), 201.44 ($\Delta\nu_{1/2}$ = 421 Hz), 78.71 ($\Delta\nu_{1/2}$ = 1750 Hz). Anal. Calcd for $C_{19}H_{31}N_5W$: C, 44.46; H, 6.09; N, 13.64. Found: C, 43.99; H, 5.86; N, 13.69.

Preparation of Mo[N(2,6-Pr$^i_2$C$_6$H$_3$)]$_2$(dpma) (4). A solution of Li_2dpma (1.001 g, 4.97 mmol) in 25 mL of ether was cooled to near frozen. This cold solution was added to $Cl_2Mo(Ndip)_2$(dme) (3.038 g, 5.00 mmol) in 25 mL of ether. The resulting solution was allowed to warm to box temperature and stirred overnight. Lithium chloride was filtered off, and ether was removed in vacuo. The resulting brown solid was recrystallized from ether/pentane, which gave **4** as a tan solid in 35% yield (1.10 g, 1.74 mmol). ^{1}H NMR (benzene-d_6): δ = 6.93−7.02 (m, 6H), 6.91 (m, 2H), 6.40 (m, 2H), 6.26 (m, 2H), 4.43 (d, J = 13.0 Hz, 2H), 3.90 (h, J = 6.7 Hz, 2H), 3.46 (d, J = 13.0 Hz, 2H), 3.18 (h, J = 6.7 Hz, 2H), 2.23 (s, 3H), 1.05 (d, J = 6.1 Hz, 9H), 1.04 (d, J = 6.1 Hz, 9H). ^{13}C NMR (benzene-d_6): δ = 153.22, 151.90, 147.91, 143.43, 139.20, 131.26, 129.55, 128.29, 128.29, 128.19, 127.81, 126.65, 122.95, 122.35, 111.06, 110.99, 105.84, 60.56, 45.46, 28.88, 28.80, 23.58, 23.42. ^{14}N NMR (benzene-d_6): δ = 429.32 ($\Delta\nu_{1/2}$ = 648 Hz), 205.85 ($\Delta\nu_{1/2}$ = 895 Hz), 42.49 ($\Delta\nu_{1/2}$ = 3132 Hz). Anal. Calcd for $C_{35}H_{47}N_5Mo$: C, 66.34; H, 7.48; N, 11.05. Found: C, 66.39; H, 7.42; N, 11.03.

General Considerations for Single-Crystal X-ray Diffraction. Single crystals of **1**−**4** were grown at −35 °C in an MBraun inert atmosphere glovebox. All but a small portion of the mother liquor was removed, and the crystals were removed from the glovebox in a sealed vial. The crystals were rapidly coated in Paratone N and mounted on a glass fiber. The mounted crystal was placed under a cold stream of nitrogen from an Oxford "Cryostream" low-temperature device. Data were collected on a Bruker-AXS, Inc., SMART CCD diffractometer utilizing a PC running Windows NT. The data collection was done on a Bruker-AXS, Inc., 3-circle goniometer (χ set to 54.78°). The source was a water-cooled Mo X-ray tube (λ = 0.71073 Å) operating at 50 kV/40 mA. A single-crystal graphite monochromator selected the wavelength of light prior to being collimated. The cell was determined using $\omega-\theta$ scans (−0.3° scan width) with 3 sets of 20 frames. The initial cell was found by repeated least squares and Bravais lattice analysis. Full data sets were collected using $\omega-\theta$ scans in four runs. The fourth run duplicates the first 50 frames of the first run to allow analysis of peak intensity changes resulting from crystal degradation; no correction was necessary for any of the structures reported. Absorption corrections were applied to the data. Using the initial cell, data were integrated to *hkl*/intensity data using the Bruker-AXS, Inc., program package SAINT. The final unit cell was determined by SAINT using all the observed data. The structures were solved and refined using the SHELXTL program developed by G. M. Sheldrick and Bruker-AXS, Inc. A full listing of atomic

(57) Schoettel, G.; Kress, J.; Osborn, J. A. *J. Chem. Soc., Chem. Commun.* **1989**, 1062−1063.

Table 3. Data from the Single Crystal X-ray Diffraction Experiments for Compounds **1**−**4**

	Cr(NBu^t)$_2$(dpma) (**1**)	Mo(NBu^t)$_2$(dpma) (**2**)	W(NBu^t)$_2$(dpma) (**3**)	Mo[N(2,6-Pr$^i_2$C$_6$H$_3$)]$_2$(dpma) (**4**)
empirical formula	$C_{19}H_{31}CrN_5$	$C_{19}H_{31}MoN_5$	$C_{19}H_{31}N_5W$	$C_{35}H_{47}MoN_5$
fw	381.49	425.43	513.34	633.72
temp/K	293(2)	293(2)	293(2)	293(2)
crystal system	monoclinic	monoclinic	monoclinic	orthorhombic
space group	*P*2(1)/*n*	*P*2(1)/*n*	*P*2(1)/*n*	*Fdd*2
a/Å	10.2007(2)	9.451(5)	9.4181(11)	19.415(5)
b/Å	9.4695(3)	10.175(5)	10.2171(12)	61.473(17)
c/Å	21.7312(5)	22.217(11)	22.190(3)	11.280(3)
β/deg	94.638(2)	93.569(9)	93.271(2)	
V/Å^3	2092.26(9)	2132.4(17)	2131.8(4)	13463(6)
Z	4	4	4	16
d(calc)/Mg m^{-3}	1.211	1.325	1.599	1.251
abs coeff/mm^{-1}	0.557	0.626	5.429	0.419
θ range for data/deg	1.88−28.24	1.84−23.32	1.84−23.26	1.32−23.33
data/params	4936/227	3082/227	3074/227	4654/379
GOF on F^2	0.929	0.931	1.090	0.977
R indices [$I > 2\sigma(I)$]	R1 = 0.0433, wR2 = 0.0961	R1 = 0.0723, wR2 = 0.1020	R1 = 0.0192, wR2 = 0.0466	R1 = 0.0431, wR2 = 0.0886
R indices (all data)	R1 = 0.0853, wR2 = 0.1071	R1 = 0.1697, wR2 = 0.1225	R1 = 0.0212, wR2 = 0.0473	R1 = 0.0673, wR2 = 0.0953

coordinates, bond lengths, bond angles, and thermal parameters for all the structures has been deposited at the Cambridge Crystallographic Data Centre and can be found in the Supporting Information. Additional data pertaining to the collection and processing of the four structures can be found in Table 3. In Table 3, $R1 = \sum||F_o| - |F_c||/\sum|F_o|$ and $wR2 = \{\sum w(F_o^2 - F_c^2)^2/\sum w(F_o^2)^2\}^{1/2}$. A partial listing of geometrical parameters for all four data sets may be found in Table 1 (see Figure 2 for labeling scheme).

Acknowledgment. The authors appreciate the financial support of the Office of Naval Research (Young Investigator Program), Petroleum Research Fund administered by the American Chemical Society, Department of Energy—Defense Programs, and Michigan State University. J.T.C. thanks MSU for Brubaker and Dye Fellowships. The authors thank Seth N. Brown for helpful comments on an early version of this manuscript.

Supporting Information Available: Tables of data on the X-ray diffraction studies. Full ^{14}N NMR spectra for compounds **1**−**4**. This material is available free of charge via the Internet at http://pubs.acs.org.

IC049644O